ORNL-TM-5203
ENDF-227

NNCSC

SB2. Experiment on Secondary Gamma-Ray Production Cross Sections Arising from Thermal-Neutron Capture in Each of 14 Different Elements Plus a Stainless Steel

R. E. Maerker

36 pgs

OAK RIDGE NATIONAL LABORATORY
OPERATED BY UNION CARBIDE CORPORATION • FOR THE U.S. ATOMIC ENERGY COMMISSION

Printed in the United States of America. Available from
National Technical Information Service
U.S. Department of Commerce
5285 Port Royal Road, Springfield, Virginia 22161
Price: Printed Copy $5.00; Microfiche $2.25

ORNL-TM-5203
ENDF-227

Contract No. W-7405-eng-26

Neutron Physics Division

SB2. Experiment on Secondary Gamma-Ray Production Cross Sections Arising from Thermal-Neutron Capture in Each of 14 Different Elements Plus a Stainless Steel

R. E. Maerker

Reference: R. E. Maerker and F. J. Muckenthaler, "Gamma-Ray Spectra Arising from Thermal-Neutron Capture in Elements Found in Soil, Concretes, and Structural Materials", ORNL-4382 (1969).

JANUARY 1976

OAK RIDGE NATIONAL LABORATORY
Oak Ridge, Tennessee 37830
operated by
Union Carbide Corporation
for the
U.S. ENERGY RESEARCH AND DEVELOPMENT ADMINISTRATION

Abstract

The experimental and calculational details for a CSEWG integral data testing shielding experiment are presented. This particular experiment measured the secondary gamma-ray production cross sections arising from thermal-neutron capture in iron, nitrogen, sodium, aluminum, copper, titanium, calcium, potassium, chlorine, silicon, nickel, zinc, barium, sulfur and a type 321 stainless steel.

Description

Gamma-ray production cross sections arising from thermal-neutron capture in iron, stainless steel, nitrogen, and sodium in 0.5-MeV bins, obtained from gamma-ray spectral measurements described in the reference, were originally collated and documented in SDT6*. The present document supplements these results with additional data on aluminum, copper, titanium, calcium, potassium, chlorine, silicon, nickel, zinc, barium and sulfur. All the measurements were made at the Oak Ridge National Laboratory Tower Shielding Facility using a carefully calibrated 5 x 5 in. NaI(Tℓ) detector in good geometry. The experimental arrangement is shown in Fig. 1. The resulting reduced spectral intensities in photons per 100 captures were summed over 0.5-MeV intervals and converted to units of millibarns per capture by using handbook values of the radiative capture cross section at 0.0253 eV.

Results

The experimental results for all 14 elements plus the stainless steel are presented in Tables 1 through 15. Note that they are given for gamma-ray energies of $\sim$ 1 MeV and greater. The estimated accuracy is $\pm$ 15% and contributions from both discrete and continuum gamma rays are included in these results.

Method of Calculation

No transport calculations are necessary for this benchmark, hence model description, atom densities, etc. are not needed. Calculations could simply consist of summing the thermal-neutron absolute capture spectra over appropriate energy intervals; however, it is recommended that a "standard" ENDF/B photon production group averaging code such as LAPHANO (written by Los Alamos) or LAPHFOR (Oak Ridge's modified version of LAPHANO) be used to accomplish this task.

The input for LAPHANO or LAPHFOR, for example, is relatively straight-forward. Note the following input items:

---

*SB2 supercedes SDT6 in the new shielding benchmark series (1976).

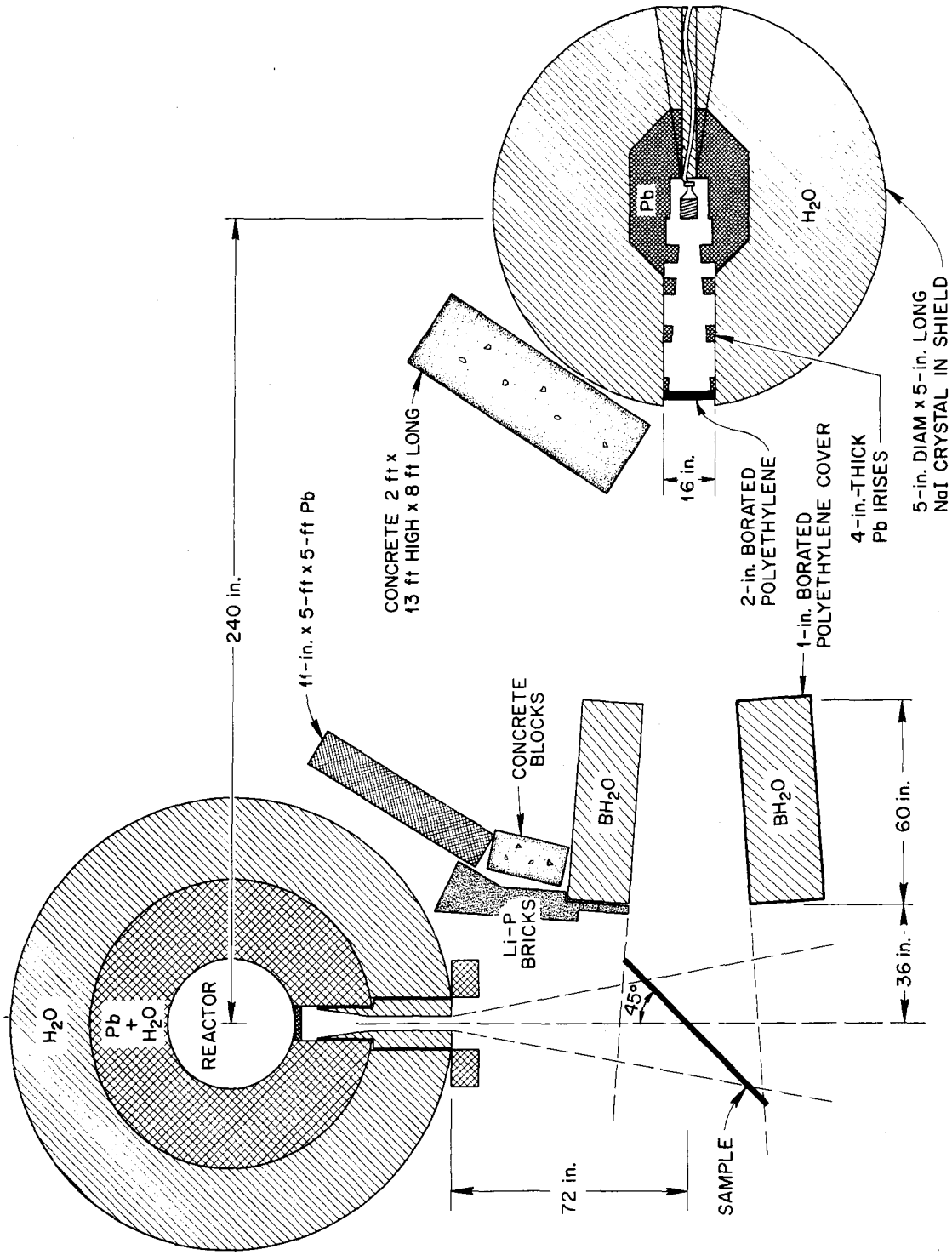

Fig. 1. Schematic Diagram of Geometry for Thermal-Neutron Capture Gamma-Ray Experiments.

NGG - number of gamma groups for each element is determined from Tables 1-15.

NGF - number of neutron fine groups - 1.

NBF - number of neutron broad groups - 1.

All flags for numbers of nuclides, mixtures, zones, etc. are set for one material, one mixture, one zone with radius = 1.0, etc. A single MT number equal 102 is specified. The gamma bounds for each element are given in the Tables and the two boundaries of the neutron fine group are those of the broad group, namely 0.02531 eV and 0.02529 eV. The single value of the neutron weighting function is 1.0. Note that the production cross sections are outputted in units of barns**.

Method of Reporting

The calculational results should be tabulated as shown in Tables 16-30.

**Acknowledgments should be made to R. J. LaBauve of Los Alamos Scientific Laboratory and W. E. Ford III of Oak Ridge National Laboratory for providing the general description of the input to the LAPHANO and LAPHFOR processing codes.

Table 1

Gamma-ray production cross sections arising from thermal-neutron capture in iron are the following, in millibarns at 0.0253 eV.

Gamma-Ray Energy Interval (MeV)*	Cross Section (mb)
1.15 - 1.5	126
1.5 - 2.0	455
2.0 - 2.5	99
2.5 - 3.0	152
3.0 - 3.5	233
3.5 - 4.0	88
4.0 - 4.5	182
4.5 - 5.0	83
5.0 - 5.5	25
5.5 - 6.0	250
6.0 - 6.5	255
6.5 - 7.0	13
7.0 - 7.5	139
7.5 - 8.0	1280
8.0 - 9.0	20
$\geq$ 9.0	83

*Upper energy limit of each group not included in summation.

Table 2

Gamma-ray production cross sections arising from thermal-neutron capture in stainless steel (67.4 weight percent iron, 18.3 weight percent chromium, 9.7 weight percent nickel, 1.5 weight percent manganese, 0.3 weight percent cobalt, and the remainder may be neglected) are the following, in millibarns at 0.0253 eV.

Gamma-Ray Energy Interval (MeV)*	Cross Section (mb)
1.0 - 1.5	442
1.5 - 2.0	355
2.0 - 2.5	186
2.5 - 3.0	134
3.0 - 3.5	226
3.5 - 4.0	113
4.0 - 4.5	177
4.5 - 5.0	98
5.0 - 5.5	107
5.5 - 6.0	287
6.0 - 6.5	229
6.5 - 7.0	125
7.0 - 7.5	259
7.5 - 8.0	1025
8.0 - 8.5	110
8.5 - 9.0	372
9.0 - 9.5	58
9.5 - 10.0	55
$\geq$ 10.0	0

*Upper energy limit of each group not included in summation.

Table 3

Gamma-ray production cross sections arising from thermal-neutron capture in nitrogen are the following, in millibarns at 0.0253 eV.

Gamma-Ray Energy Interval (MeV)*	Cross Section (mb)
1.0 - 1.5	0
1.5 - 2.0	30.0
2.0 - 2.5	0
2.5 - 3.0	6.4
3.0 - 3.5	0
3.5 - 4.0	22.8
4.0 - 4.5	0
4.5 - 5.0	13.4
5.0 - 5.5	43.3
5.5 - 6.0	25.2
6.0 - 6.5	15.2
6.5 - 7.0	0
7.0 - 7.5	7.8
7.5 - 8.0	0
8.0 - 8.5	3.5
8.5 - 9.0	0.17
9.0 - 9.5	1.6
9.5 - 10.0	0
10.0 - 10.5	0
10.5 - 11.0	11.0
$\geq$ 11.0	0

*Upper energy limit of each group not included in summation.

Table 4

Gamma-ray production cross sections arising from thermal-neutron capture in sodium are the following, in millibarns at 0.0253 eV.

Gamma-Ray Energy Interval (MeV)*	Cross Section (mb)
1.0 - 1.5	79†
1.5 - 2.0	76
2.0 - 2.5	143
2.5 - 3.0	254†
3.0 - 3.5	76
3.5 - 4.0	182
4.0 - 4.5	34
4.5 - 5.0	14
5.0 - 5.5	12
5.5 - 6.0	31
6.0 - 6.5	115
$\geq$ 6.5	0

*Upper energy limit of each group not included in summation.

†Does not include the contribution of 534 mb from ^{24}Na activation (i.e., gamma rays resulting from decay to ^{24}Mg).

Table 5

Gamma-ray production cross sections arising from thermal-neutron capture in aluminum are the following, in millibarns at 0.0253 eV.

Gamma-Ray Energy Interval (MeV)*	Cross Section (mb)
0.98 - 1.5	43
1.5 - 2.0	24†
2.0 - 2.5	31
2.5 - 3.0	48
3.0 - 3.5	37
3.5 - 4.0	34
4.0 - 4.5	38
4.5 - 5.0	41
5.0 - 5.5	16
5.5 - 6.0	6.6
6.0 - 6.5	14
6.5 - 7.0	5.1
7.0 - 7.5	1.6
7.5 - 8.0	76
$\geq$ 8.0	0

*Upper energy limit of each group not included in summation.

†Does not include the contribution of 234 mb from ^{28}Al activation (i.e., gamma rays resulting from decay to ^{28}Si).

Table 6

Gamma-ray production cross sections arising from thermal-neutron capture in copper are the following, in millibarns at 0.0253 eV.

Gamma-Ray Energy Interval (MeV)*	Cross Section (mb)
1.0 - 1.5	501
1.5 - 2.0	518
2.0 - 2.5	246
2.5 - 3.0	324
3.0 - 3.5	317
3.5 - 4.0	290
4.0 - 4.5	378
4.5 - 5.0	159
5.0 - 5.5	324
5.5 - 6.0	74
6.0 - 6.5	183
6.5 - 7.0	349
7.0 - 7.5	534
7.5 - 8.0	1510
$\geq$ 8.0	0

*Upper energy limit of each group not included in summation.

Table 7

Gamma-ray production cross sections arising from thermal-neutron capture in titanium are the following, in millibarns at 0.0253 eV.

Gamma-Ray Energy Interval (MeV)*	Cross Section (mb)
1.25 - 1.5	4730
1.5 - 2.0	1590
2.0 - 2.5	203
2.5 - 3.0	282
3.0 - 3.5	350
3.5 - 4.0	260
4.0 - 4.5	40
4.5 - 5.0	537
5.0 - 5.5	23
5.5 - 6.0	56
6.0 - 6.5	1870
6.5 - 7.0	3160
7.0 - 7.5	51
7.5 - 8.0	10
8.0 - 8.5	18
8.5 - 9.0	0
$\geq$ 9.0	12

*Upper energy limit of each group not included in summation.

Table 8

Gamma-ray production cross sections arising from thermal-neutron capture in calcium are the following, in millibarns at 0.0253 eV.

Gamma-Ray Energy Interval (MeV)*	Cross Section (mb)
1.06 - 1.5	90
1.5 - 2.5	522
2.5 - 3.0	62
3.0 - 3.5	34
3.5 - 4.0	58
4.0 - 4.5	84
4.5 - 5.0	28
5.0 - 5.5	11
5.5 - 6.0	52
6.0 - 6.5	173
$\geq$ 6.5	0

*Upper energy limit of each group not included in summation.

Table 9

Gamma-ray production cross sections arising from thermal-neutron capture in potassium are the following, in millibarns at 0.0253 eV.

Gamma-Ray Energy Interval (MeV)*	Cross Section (mb)
1.0 - 1.5	689
1.5 - 2.0	636
2.0 - 2.5	770
2.5 - 3.0	486
3.0 - 3.5	346
3.5 - 4.0	480
4.0 - 4.5	418
4.5 - 5.0	159
5.0 - 5.5	335
5.5 - 6.0	358
6.0 - 6.5	20
6.5 - 7.0	45
7.0 - 7.5	9.3
7.5 - 8.0	117
$\geq$ 8.0	0

*Upper energy limit of each group not included in summation.

Table 10

Gamma-ray production cross sections arising from thermal-neutron capture in chlorine are the following, in millibarns at 0.0253 eV.

Gamma-Ray Energy Interval (MeV)*	Cross Section (mb)
1.0 - 1.5	13500
1.5 - 2.0	13600
2.0 - 2.5	4280
2.5 - 3.0	5770
3.0 - 3.5	3680
3.5 - 4.0	2720
4.0 - 4.5	1940
4.5 - 5.0	2690
5.0 - 5.5	1020
5.5 - 6.0	3500
6.0 - 6.5	7840
6.5 - 7.0	5470
7.0 - 7.5	3710
7.5 - 8.0	2990
8.0 - 8.5	0
8.5 - 9.0	960
$\geq$ 9.0	0

*Upper energy limit of each group not included in summation.

Table 11

Gamma-ray production cross sections arising from thermal-neutron capture in silicon are the following, in millibarns at 0.0253 eV.

Gamma-Ray Energy Interval (MeV)*	Cross Section (mb)
1.0 - 1.5	23.3
1.5 - 2.0	0
2.0 - 2.5	35.0
2.5 - 3.0	7.0
3.0 - 3.5	8.2
3.5 - 4.0	117
4.0 - 4.5	1.2
4.5 - 5.0	107
5.0 - 5.5	9.8
5.5 - 6.0	0.3
6.0 - 6.5	18.6
6.5 - 7.0	1.2
7.0 - 7.5	14.8
7.5 - 8.0	0
8.0 - 8.5	3.4
$\geq$ 8.5	0

*Upper energy limit of each group not included in summation.

Table 12

Gamma-ray production cross sections arising from thermal-neutron capture in nickel are the following, in millibarns at 0.0253 eV.

Gamma-Ray Energy Interval (MeV)*	Cross Section (mb)
1.0 - 1.5	290
1.5 - 2.0	128
2.0 - 2.5	106
2.5 - 3.0	150
3.0 - 3.5	97
3.5 - 4.0	77
4.0 - 4.5	53
4.5 - 5.0	63
5.0 - 5.5	165
5.5 - 6.0	208
6.0 - 6.5	203
6.5 - 7.0	542
7.0 - 7.5	140
7.5 - 8.0	504
8.0 - 8.5	368
8.5 - 9.0	2320
$\geq$ 9.0	0

*Upper energy limit of each group not included in summation.

Table 13

Gamma-ray production cross sections arising from thermal-neutron capture in zinc are the following, in millibarns at 0.0253 eV.

Gamma-Ray Energy Interval (MeV)*	Cross Section (mb)
1.0 - 1.5	509
1.5 - 2.0	377
2.0 - 2.5	261
2.5 - 3.0	187
3.0 - 3.5	234
3.5 - 4.0	142
4.0 - 4.5	148
4.5 - 5.0	143
5.0 - 5.5	127
5.5 - 6.0	107
6.0 - 6.5	76
6.5 - 7.0	135
7.0 - 7.5	56
7.5 - 8.0	145
8.0 - 8.5	10
8.5 - 9.0	1
9.0 - 9.5	12
$\geq$ 9.5	0

*Upper energy limit of each group not included in summation.

Table 14

Gamma-ray production cross sections arising from thermal-neutron capture in barium are the following, in millibarns at 0.0253 eV.

Gamma-Ray Energy Interval (MeV)*	Cross Section (mb)
1.0 - 1.5	723
1.5 - 2.0	498
2.0 - 2.5	412
2.5 - 3.0	292
3.0 - 3.5	211
3.5 - 4.0	192
4.0 - 4.5	337
4.5 - 5.0	151
5.0 - 5.5	91
5.5 - 6.0	114
6.0 - 6.5	48
6.5 - 7.0	12
7.0 - 8.0	24
8.0 - 8.5	4
8.5 - 9.0	2
9.0 - 9.5	5
$\geq$ 9.5	0

*Upper energy limit of each group not included in summation.

Table 15

Gamma-ray production cross sections arising from thermal-neutron capture in sulfur are the following, in millibarns at 0.0253 eV.

Gamma-Ray Energy Interval (MeV)*	Cross Section (mb)
1.0 - 1.5	8.8
1.5 - 2.0	19
2.0 - 2.5	228
2.5 - 3.0	119
3.0 - 3.5	153
3.5 - 4.0	16
4.0 - 4.5	36
4.5 - 5.0	80
5.0 - 5.5	322
5.5 - 6.0	20
6.0 - 6.5	2.1
6.5 - 7.0	5.2
7.0 - 7.5	5.2
7.5 - 8.0	18
8.0 - 8.5	2.6
8.5 - 9.0	10
$\geq$ 9.0	0

*Upper energy limit of each group not included in summation.

Table 16

Report sheet for gamma-ray production cross sections arising from thermal-neutron capture in iron.

Gamma-Ray Energy Interval (MeV)*	Cross Section at 0.0253 eV (mb)
1.15 - 1.5	
1.5 - 2.0	
2.0 - 2.5	
2.5 - 3.0	
3.0 - 3.5	
3.5 - 4.0	
4.0 - 4.5	
4.5 - 5.0	
5.0 - 5.5	
5.5 - 6.0	
6.0 - 6.5	
6.5 - 7.0	
7.0 - 7.5	
7.5 - 8.0	
8.0 - 9.0	
$\geq$ 9.0	

*Do not include upper energy limit of each group in summation.

Table 17

Report sheet for gamma-ray production cross sections arising from thermal-neutron capture in stainless steel.

Gamma-Ray Energy Interval (MeV)*	Cross Section at 0.0253 eV (mb)
1.0 - 1.5	
1.5 - 2.0	
2.0 - 2.5	
2.5 - 3.0	
3.0 - 3.5	
3.5 - 4.0	
4.0 - 4.5	
4.5 - 5.0	
5.0 - 5.5	
5.5 - 6.0	
6.0 - 6.5	
6.5 - 7.0	
7.0 - 7.5	
7.5 - 8.0	
8.0 - 8.5	
8.5 - 9.0	
9.0 - 9.5	
9.5 - 10.0	
$\geq$ 10.0	

*Do not include upper energy limit of each group in summation.

Table 18

Report sheet for gamma-ray production cross sections arising from thermal capture in nitrogen.

Gamma-Ray Energy Interval (MeV)*	Cross Section at 0.0253 eV (mb)
1.0 - 1.5	
1.5 - 2.0	
2.0 - 2.5	
2.5 - 3.0	
3.0 - 3.5	
3.5 - 4.0	
4.0 - 4.5	
4.5 - 5.0	
5.0 - 5.5	
5.5 - 6.0	
6.0 - 6.5	
6.5 - 7.0	
7.0 - 7.5	
7.5 - 8.0	
8.0 - 8.5	
8.5 - 9.0	
9.0 - 9.5	
9.5 - .0.0	
10.0 - 10.5	
10.5 - 11.0	
$\geq$ 11.0	

*Do not include upper energy limit of each group in summation.

Table 19

Report sheet for gamma-ray production cross sections arising from thermal-neutron capture in sodium.

Gamma-Ray Energy Interval (MeV)*	Cross Section at 0.0253 eV (mb)†
1.0 - 1.5	
1.5 - 2.0	
2.0 - 2.5	
2.5 - 3.0	
3.0 - 3.5	
3.5 - 4.0	
4.0 - 4.5	
4.5 - 5.0	
5.0 - 5.5	
5.5 - 6.0	
6.0 - 6.5	
$\geq$ 6.5	

*Do not include upper energy limit of each group in summation.

†Do not include the contribution from ^{24}Na activation (i.e., gamma rays resulting from decay to ^{24}Mg).

Table 20

Report sheet for gamma-ray production cross sections arising from thermal-neutron capture in aluminum.

Gamma-Ray Energy Interval (MeV)*	Cross Section (mb) †
0.98 - 1.5	
1.5 - 2.0	
2.0 - 2.5	
2.5 - 3.0	
3.0 - 3.5	
3.5 - 4.0	
4.0 - 4.5	
4.5 - 5.0	
5.0 - 5.5	
5.5 - 6.0	
6.0 - 6.5	
6.5 - 7.0	
7.0 - 7.5	
7.5 - 8.0	
$\geq$ 8.0	

*Upper energy limit of each group not included in summation.

†Do not include the contribution from ^{28}Al activation (i.e., gamma rays resulting from decay to ^{28}Si).

Table 21

Report sheet for gamma-ray production cross sections arising from thermal-neutron capture in copper.

Gamma-Ray Energy Interval (MeV)*	Cross Section (mb)
1.0 - 1.5	
1.5 - 2.0	
2.0 - 2.5	
2.5 - 3.0	
3.0 - 3.5	
3.5 - 4.0	
4.0 - 4.5	
4.5 - 5.0	
5.0 - 5.5	
5.5 - 6.0	
6.0 - 6.5	
6.5 - 7.0	
7.0 - 7.5	
7.5 - 8.0	
$\geq$ 8.0	

*Upper energy limit of each group not included in summation.

Table 22

Report sheet for gamma-ray production cross sections arising from thermal-neutron capture in titanium.

Gamma-Ray Energy Interval (MeV)*	Cross Section (mb)
1.25 - 1.5	
1.5 - 2.0	
2.0 - 2.5	
2.5 - 3.0	
3.0 - 3.5	
3.5 - 4.0	
4.0 - 4.5	
4.5 - 5.0	
5.0 - 5.5	
5.5 - 6.0	
6.0 - 6.5	
6.5 - 7.0	
7.0 - 7.5	
7.5 - 8.0	
8.0 - 8.5	
8.5 - 9.0	
$\geq$ 9.0	

*Upper energy limit of each group not included in summation.

Table 23

Report sheet for gamma-ray production cross sections arising from thermal-neutron capture in calcium.

Gamma-Ray Energy Interval (MeV)*	Cross Section (mb)
1.06 - 1.5	
1.5 - 2.5	
2.5 - 3.0	
3.0 - 3.5	
3.5 - 4.0	
4.0 - 4.5	
4.5 - 5.0	
5.0 - 5.5	
5.5 - 6.0	
6.0 - 6.5	
$\geq$ 6.5	

*Upper energy limit of each group not included in summation.

Table 24

Report sheet for gamma-ray production cross sections arising from thermal-neutron capture in potassium.

Gamma-Ray Energy Interval (MeV)*	Cross Section (mb)
1.0 - 1.5	
1.5 - 2.0	
2.0 - 2.5	
2.5 - 3.0	
3.0 - 3.5	
3.5 - 4.0	
4.0 - 4.5	
4.5 - 5.0	
5.0 - 5.5	
5.5 - 6.0	
6.0 - 6.5	
6.5 - 7.0	
7.0 - 7.5	
7.5 - 8.0	
$\geq$ 8.0	

*Upper energy limit of each group not included in summation.

Table 25

Report sheet for gamma-ray production cross sections arising from thermal-neutron capture in chlorine.

Gamma-Ray Energy Interval (MeV)*	Cross Section (mb)
1.0 - 1.5	
1.5 - 2.0	
2.0 - 2.5	
2.5 - 3.0	
3.0 - 3.5	
3.5 - 4.0	
4.0 - 4.5	
4.5 - 5.0	
5.0 - 5.5	
5.5 - 6.0	
6.0 - 6.5	
6.5 - 7.0	
7.0 - 7.5	
7.5 - 8.0	
8.0 - 8.5	
8.5 - 9.0	
$\geq$ 9.0	

*Upper energy limit of each group not included in summation.

Table 26

Report sheet for gamma-ray production cross sections arising from thermal-neutron capture in silicon.

Gamma-Ray Energy Interval (MeV)*	Cross Section (mb)
1.0 - 1.5	
1.5 - 2.0	
2.0 - 2.5	
2.5 - 3.0	
3.0 - 3.5	
3.5 - 4.0	
4.0 - 4.5	
4.5 - 5.0	
5.0 - 5.5	
5.5 - 6.0	
6.0 - 6.5	
6.5 - 7.0	
7.0 - 7.5	
7.5 - 8.0	
8.0 - 8.5	
$\geq$ 8.5	

*Upper energy limit of each group not included in summation.

Table 27

Report sheet for gamma-ray production cross sections arising from thermal-neutron capture in nickel.

Gamma-Ray Energy Interval (MeV)*	Cross Section (mb)
1.0 - 1.5	
1.5 - 2.0	
2.0 - 2.5	
2.5 - 3.0	
3.0 - 3.5	
3.5 - 4.0	
4.0 - 4.5	
4.5 - 5.0	
5.0 - 5.5	
5.5 - 6.0	
6.0 - 6.5	
6.5 - 7.0	
7.0 - 7.5	
7.5 - 8.0	
8.0 - 8.5	
8.5 - 9.0	
$\geq$ 9.0	

*Upper energy limit of each group not included in summation.

Table 28

Report sheet for gamma-ray production cross sections arising from thermal-neutron capture in zinc.

Gamma-Ray Energy Interval (MeV)*	Cross Section (mb)
1.0 - 1.5	
1.5 - 2.0	
2.0 - 2.5	
2.5 - 3.0	
3.0 - 3.5	
3.5 - 4.0	
4.0 - 4.5	
4.5 - 5.0	
5.0 - 5.5	
5.5 - 6.0	
6.0 - 6.5	
6.5 - 7.0	
7.0 - 7.5	
7.5 - 8.0	
8.0 - 8.5	
8.5 - 9.0	
9.0 - 9.5	
$\geq$ 9.5	

*Upper energy limit of each group not included in summation.

Table 29

Report sheet for gamma-ray production cross sections arising from thermal-neutron capture in barium.

Gamma-Ray Energy Interval (MeV)*	Cross Section (mb)
1.0 - 1.5	
1.5 - 2.0	
2.0 - 2.5	
2.5 - 3.0	
3.0 - 3.5	
3.5 - 4.0	
4.0 - 4.5	
4.5 - 5.0	
5.0 - 5.5	
5.5 - 6.0	
6.0 - 6.5	
6.5 - 7.0	
7.0 - 8.0	
8.0 - 8.5	
8.5 - 9.0	
9.0 - 9.5	
$\geq$ 9.5	

*Upper energy limit of each group not included in summation.

Table 30

Report sheet for gamma-ray production cross sections arising from thermal-neutron capture in sulfur.

Gamma-Ray Energy Interval (MeV)*	Cross Section (mb)
1.0 - 1.5	
1.5 - 2.0	
2.0 - 2.5	
2.5 - 3.0	
3.0 - 3.5	
3.5 - 4.0	
4.0 - 4.5	
4.5 - 5.0	
5.0 - 5.5	
5.5 - 6.0	
6.0 - 6.5	
6.5 - 7.0	
7.0 - 7.5	
7.5 - 8.0	
8.0 - 8.5	
8.5 - 9.0	
$\geq$ 9.0	

*Upper energy limit of each group not included in summation.

ORNL-TM-5203
ENDF-227

INTERNAL DISTRIBUTION

1-3. L. S. Abbott
4-8. C. E. Clifford
9. G. F. Flanagan
10. W. E. Ford III
11. H. Goldstein (Consultant)
12. W. O. Harms
13. R. E. Maerker
14. F. C. Maienschein
15. F. J. Muckenthaler
16. F. R. Mynatt
17. E. M. Oblow
18. F. G. Perey
19. R. W. Roussin
20. D. B. Trauger
21. D. K. Trubey
22. C. R. Weisbin
23. G. E. Whitesides
24. A. Zucker
25-44. RSIC
45. W. W. Havens (Consultant)
46. A. F. Henry (Consultant)
47. P. F. Fox (Consultant)
48-49. Central Research Library
50. ORNL Y-12 Technical Library
Document Reference Section
51-52. Laboratory Records Dept.
53. Laboratory Records ORNL RC
54. ORNL Patent Office

EXTERNAL DISTRIBUTION

55. Martin Becker, Rensselaer Polytechnic Institute, Tibbits Ave., Troy, N. Y. 12181
56. N. Francis, Knolls Atomic Power Laboratory, Schenectady, N. Y. 12301
57. R. A. Grimesey, Idaho Nuclear Corp., P. O. Box 1845, Idaho Falls, Idaho 83401
58. W. H. Hannum, Div. of Reactor Research and Development, Safety, ERDA, Washington, D. C. 20545
59. P. B. Hemmig, Div. of Reactor Research and Development, Reactor Physics Branch, ERDA, Washington, D. C. 20545
60. L. Harris, Science Applications Inc., P. O. Box 2351, La Jolla, California 92037
61. M. H. Kalos, Courant Institute of Mathematical Sciences, New York University, 251 Mercer Street, New York, N. Y. 10012
62. R. J. LaBauve, Los Alamos Scientific Laboratory, P. O. Box 1663, Los Alamos, New Mexico 87544
63. Leona Stewart, Los Alamos Scientific Laboratory, P. O. Box 1663, Los Alamos, New Mexico 87544
64. Duane Marr, WADCO, P. O. Box 1970, Richland, Washington 99352
65. R. J. Howerton, Lawrence Livermore Laboratory, P. O. Box 808, Livermore, California 94550
66. E. A. Straker, Science Applications, Inc., P. O. Box 2351, La Jolla, California 92037
67-86. Sol Pearlstein, NNCSC, Brookhaven National Laboratory, Upton, N. Y. 11973
87. E. M. Bohn, Argonne National Laboratory, 9700 Cass Avenue, Argonne, Illinois 60439
88. Dr. John Butler, Bldg. B21, United Kingdom Atomic Energy Authority, AEE Winfrith, Dorchester, Dorset, England
89. C. Devillers, DPRMA/SERMA, B. P. 2, CEN Saclay, 91190 Gif Sur Yvette, France

90. Dr. Carlo Ponti, CCR Curatom, 21027 ISPRA(Varese), Italy
91. Dr. G. Hehn, Institut Fur Kernenergetik, Der Universitat, 7000 Stuttgart 80, Pfaffenwaldring 31, Germany
92. Tomas Lefvert, Research Institute of National Defense, FOA 212, FACK, S-10450, Stockholm 80, Sweden
93. Makato Akanuma, Computing Center, Div. of Reactor Eng., Japan Atomic Energy Research Institute, Tokai Research Establishment, Tokai-Mura, Naka-Gun, Ibaraki-Ken, Japan
94-120. Technical Information Center (TIC)
121. Research and Technical Support Division